Applied Surface Science 346 (2015) 477–483

Contents lists available at ScienceDirect

Applied Surface Science

journal homepage: www.elsevier.com/locate/apsusc

Novel method for synthesis of silver nanoparticles and their application on wool

Majid Nasiri Boroumand[a], Majid Montazer[b], Frank Simon[c], Jolanta Liesiene[d], Zoran Šaponjic[e], Victoria Dutschk[f,*]

[a] Shahid Bahonar University of Kerman, Kerman, Iran
[b] Amirkabir University of Technology, Tehran, Iran
[c] Leibniz-Institut für Polymerforschung Dresden e.V., Dresden, Germany
[d] Faculty of Chemical Technology, Kaunas University of Technology, Kaunas, Lithuania
[e] Vinča Institute of Nuclear Sciences, University of Belgrade, Belgrade, Serbia
[f] Faculty of Engineering Technology, University of Twente, Enschede, The Netherlands

ARTICLE INFO

Article history:
Received 3 December 2014
Received in revised form 8 March 2015
Accepted 6 April 2015
Available online 14 April 2015

Keywords:
Natural dye
Silver nanoparticle
Antibacterial
Pomegranate
Wool

ABSTRACT

In this study, a new method for the synthesis of silver nanoparticles (AgNPs) suitable to impart antibacterial properties of wool fabric is proposed. AgNPs were synthesized by a biochemical reduction method. An aqueous solution of extracted dye from *Pomegranate peel* was used as a reducing agent for the synthesis of AgNPs from silver nitrate. The ratio of dye to silver nitrate concentration ($R_{Dye}/_{Ag}$ = [Dye]/[$AgNO_3$]) is the influencing factor in the synthesis of silver nanoparticles. The nanoparticles formation was followed by UV/Vis absorption spectroscopy. The size and shape of AgNPs were studied by transmission electron microscopy (TEM). The size distribution and Zetapotential of nanoparticles were evaluated using diffraction light scattering (DLS) measurements. The antibacterial potential of biosynthesized silver nanoparticles against *Escherichia coli* (*E. coli*) was examined qualitatively and quantitatively. Kinetic analysis of the bacteria reduction using AgNPs synthesized in different way was performed. AgNPs were applied on wool fabrics by exhaustion. The changes in surface morphology of wool fibers after AgNPs loading were studied using scanning electron microscopy (SEM). The amounts of silver deposited on wool fabrics at different pH and temperature were compared applying energy-dispersive X-ray spectroscopy (EDX). AgNPs loaded fabrics showed excellent antibacterial efficiency even after five washing cycles. To investigate the nature of interaction and bonding between the AgNPs and the wool substrate XPS measurements were performed.

1. Introduction

Nanotechnology increasingly attracts attention of textile industry since it opens up new possibilities for modification of the textile materials with specific end-use properties [1,2]. An important area of research in nanotechnology concerns the synthesis of nanoparticles of different chemical compositions, sizes, shapes, and controlled polydispersity [3]. Currently, there is a growing need to develop environmentally benign nanoparticle synthesis in which toxic chemicals are excluded. As a result, researchers in the field of nanoparticles synthesis and assembly have turned to biological systems for inspiration [4–8].

Silver nanoparticles are important materials that have been studied extensively. Silver has been known as a disinfectant for many years and is being used in many forms in the treatment of infectious diseases and has a broad spectrum antibacterial activity while exhibiting low toxicity towards mammalian cells [9,10].

Recently, the major research interests in textile industry have been focused on the application of AgNPs to different textile fibers for imparting antimicrobial effects [11–19]. There are several reports in which the wool fabrics have been loaded with metal nanoparticles to impart antibacterial properties [20–28].

The rind of *Punica granatum L.* (pomegranate) belongs to the family Punicaceae contains a considerable amount of tannin. The main coloring agent in the pomegranate peel is granatonine which is present in the alkaloid form N-methyl-granatonine [29]. In addition, pomegranate peel extract with an abundance of flavonoids and tannins has been shown to have a high antioxidant activity [30]. The brown dry rind of pomegranate has been

* Corresponding author. Tel.: +31 619835325.
E-mail address: v.dutschk@utwente.nl (V. Dutschk).

http://dx.doi.org/10.1016/j.apsusc.2015.04.047
0169-4332/

used as a dye from ancient time. Biological synthesis of gold nanoparticles from pomegranate was reported previously by others [31].

In this paper, we report on a facile and rapid biosynthesis of AgNPs employing an extract of pomegranate peel as a reducing agent. Synthesized AgNPs were applied to wool by exhaustion. AgNPs were characterized by UV/vis spectroscopy and TEM. Surface morphologies of wool fabrics loaded with AgNPs were studied using SEM. The antibacterial efficiency of wool fabrics modified by AgNPs against gram-positive bacterium *Staphylococcus aureus* was quantitatively evaluated. The laundering durability of the achieved bactericidal effect on *Escherichia coli* was examined.

2. Materials and methods

2.1. Materials

Silver nitrate ($AgNO_3$ extra pure, >99.8%) was purchased from Merck. Pomegranate (*P. granatum L.*) pill powder was prepared from Iranian traditional dyers. The pH was adjusted to 8 with a 0.1 M NaOH aqueous solution (Sigma–Aldrich). All the chemicals and reagents used in this study were of analytical grade. Wool fabric was supplied by Iran Merinos Co. (Iran). A nonionic surfactant, Marlipal 24/60 was kindly supplied by Sasol (Germany).

2.2. Dye extraction

10 g of pomegranate powder was placed in a round-bottom flask. 400 mL of a methanol/water solution (ratio 8:2 v/v) was added to the flask. The flasks were placed on a heating plate with a stirrer and refluxed for 15 min at the boiling point under vigorous stirring. Then, the extracts were filtered using a Whatman filter (no. 541, mesh size 22 μm). To obtain powdered material filtrate was heated in an oven at 45 °C for 24 h. The powder was kept in a refrigerator and used for further experiments.

2.3. Synthesis of AgNPs

First, an aqueous solution of 100 ppm $AgNO_3$ was prepared. The aqueous solution of extracted dye from *Pomegranate peel* was prepared by dilution of 0.2 g extracted dye in 100 mL of deionized water and stirred for 5 min at room temperature. Then, the solution was filtered using a HPLC syringe filter (0.45 μm, 25 mm). The required amounts of aqueous solutions of extracted dyes, maintaining dye to silver ratio 0.1, 1 and 10, were mixed with distilled water to a final volume of 50 mL. For the synthesis of AgNPs, 50 mL of a 100 ppm $AgNO_3$ solution was added to the aqueous solution of extracted dye at room temperature under vigorous stirring and stirred for 1 h. Water, silver and aqueous solution of extracted dye were separately adjusted to pH 8 before mixing together.

2.4. Application of AgNPs to wool fabrics

In order to scour wool fabrics before deposition of AgNPs, the fabric samples were immersed in an aqueous solution containing a nonionic surfactant Marlipal 24/60, in concentration of 1 g/L for 30 min at 50 °C and with the material to liquor ratio of 1:40. Then the samples were rinsed with distilled water and dried at 25 °C. Using a 0.1 mmol/L HNO_3, the pH value of AgNPs solutions was decreased to 5. The scoured wool sample was immersed in the solution with a material to liquor ratio of 1:50 for 24 h at 25 °C. Afterwards, the wool fabric treated was rinsed with distilled water and dried at room temperature. Effect of pH and temperature on loading of AgNPs on wool was investigated at 25, 45 and 65 °C at pH 3 and pH 5.

2.5. Characterization

The UV/vis absorption spectra of the suspended AgNPs were monitored by a Cary 100 Bio UV/vis spectrophotometer (Varian, Palo Alto, USA). Size and shape of AgNPs were analyzed by a transmission electron microscope (TEM) Libra 200 (Carl Zeiss SMT, Germany). Samples for TEM measurements were prepared by placing a 2 μL drop of solution on the carbon-coated copper grid followed by slow evaporation at room temperature. Surface morphology of the wool fabrics loaded with AgNPs was studied by a low-voltage scanning electron microscope (LV SEM) Gemini Ultra Plus (Carl Zeiss SMT Germany). The sizes of the AgNPs and their distribution were measured in dependence on pH using a Coulter LS200 particle size analyzer (Beckman Coulter, USA). The instrument was also used to determine the electrokinetic potential (Zeta potential, ζ) of AgNPs in dependence on pH values of the suspension. These experiments were performed as particle electrophoresis measurements. From the electrophoretic mobility (μ_e) measured in a constant electric field the Zeta-potential values were calculated according to the Hückel equation [32]. The elemental composition of the material was analyzed with an EDX-720/800HS EDX spectrometer (Shimadzu Europa, Germany). For determination of the isoelectric point of wool fabric, streaming potential measurements were carried-out using the electrokinetic analyzer EKA (Anton Paar, Austria). In a measuring cell, a plug of the wool sample was formed between two perforated electrodes, which were carefully platinated. An aqueous solution of 1 mmol/L KCl was pumped through the capillary system of the plug. After flushing, necessary to adjust a constant pH value of the solution, the solution was pumped through the plug in both flow directions. The applied pressure (p) was varied from 0 to 250 mbar. The electric potential between the two electrodes (U) was measured in dependence of the applied pressure. The Zeta potential value was calculated from the steaming potential (dU/dp) according the Smoluchowski equation [33]. For all samples the streaming potential was recorded in dependence on pH of aqueous solutions. The pH values of the KCl solutions were adjusted by 0.1 mol/L solutions of KOH or HCl.

X-ray photoelectron spectroscopy (XPS) was carried out by means of an Axis Ultra X-ray photoelectron spectrometer (Kratos Analytical, UK). The spectrometer is equipped with a monochromatic Al Kα ($h\nu$ = 1486.6 eV) X-ray source of 300 W at 15 kV. The kinetic energy of the photoelectrons was determined with a hemispheric analyzer set to pass energies of 160 eV for wide scan spectra and 20 eV for high-resolution spectra. During all measurements electrostatic charging of the sample was overcompensated by means of a low-energy electron source working in combination with a magnetic immersion lens. Later, all recorded peaks were shifted by the same amount which was necessary to set the C 1s peak to 285.00 eV for saturated hydrocarbons. Quantitative elemental compositions were determined from peak areas using experimentally determined sensitivity factors and the spectrometer transmission function. Spectrum background was subtracted according to Shirley [34]. High-resolution element spectra were deconvoluted by means of a computer routine (Kratos Analytical, UK). Free parameters of component peaks were their binding energy (BE), height, full width at half maximum and the Gaussian–Lorentzian ratio. In order to prevent contributions of the sample holder to the XPS spectra, all sample fabrics (2 cm × 2 cm) were prepared on a sample holder having a hole in the area where the measurements were performed.

2.6. Antibacterial test on AgNPs solutions

In order to determine antibacterial activity of synthesized AgNPs against *E. coli* a bacteriostatic agar-based test (ATCC 11229) was used and result was expressed in term of the size of inhibition zone

(in mm). Surfaces of Petri dishes, containing 15 mL Mueller–Hinton agar, were seeded individually with bacterial suspensions (equivalent to the 0.5 McFarland standard, 1.5×10^8 CFU/mL), using a sterile cotton swab. Wells were produced by punching a stainless-steel cylinder (80 mm in diameter) onto the agar plates and removing the agar. The 80 μL aliquots of each prepared sample were placed individually in the wells. The Petri dishes were incubated at 37 °C for 24 h, thereafter the zones of inhibition were determined [35].

Bactericidal kinetic was assessed without nutrient medium. For this purpose, 40 mL of AgNPs solutions (50 ppm) were inoculated with bacterial suspension at a final concentration of 10^8 CFU/mL. Then, 1 mL aliquots were removed in different time intervals, after $t = 0$, 5, 10, 20, 40 and 60 min and added to a 9 mL neutralizing solution. Total bacterial count was determined by pour plate method using casein soy peptone (CASO) agar medium [36].

The minimum bactericidal concentration (MBC) was defined as the minimum concentration of antibacterial agent that kills more than 99.9% of the first bacterial inoculated. To determine the MBC, the bacterial suspension was added to the tubes containing various concentrations of silver nano composites solutions (40, 30, 20 and 10 ppm) in Mueller–Hinton broth to reach the final concentration of about 10^8 CFU/mL. Tubes were incubated and shake at 37 °C for 24 h. 25 μL of each tube was poured on agar medium and incubated for 24 h [36].

2.7. Antibacterial test on wool fabric

A quantitative evaluation of antibacterial efficiency of AgNPs loaded wool fabrics was done against gram-negative bacteria *E. coli* (ATCC 11229). This test was carried out according to the AATCC test method 100–2004 [22]. The square specimens of $4.8 \pm .1$ cm were prepared. Each swatch was individually placed in a sterile lid of Petri dish and inoculated with 0.5 mL of bacterial suspension (10^7 CFU/mL) for 24 h. After inoculation, each sample was placed in a 40 mL solution containing saline and 2 g/L of a nonionic surfactant (Triton X-100 from Sigma–Aldrich) and was shaken vigorously for 1 min. To measure the number of bacteria at $t = 0$, the samples were placed in saline and surfactant solution as soon as possible after inoculation (zero contact time). The total bacterial count was determined by serial dilution and pour plate method using CASO-agar medium. The antibacterial efficiency of loaded samples as term of bactericidal was calculated using Equation (1):

$$E = \frac{A - B}{A} \times 100\% \quad (1)$$

where E is the percentage of bacteria reduction, A is the number of bacteria recovered from the inoculated treated test immediately after inoculation and B is the number of bacteria recovered from the inoculated treated test after 24 h [22].

2.8. Washing procedure of loaded wool samples

To check durability of antibacterial properties of AgNPs loaded wool fabric, samples were washed with a nonionic surfactant Marlipal 24/60 at 40 °C for 20 min, then rinsed with distilled water and dried at room temperature. This washing cycle was repeated five times for each sample.

3. Results and discussions

3.1. Characterization of Ag NPs

Pomegranate peel contains polyphenols that can act as a biological reducing agent. Polyphenols which have two hydroxy groups in *ortho*- or *para*-position of their phenyl rings can easily be oxidized

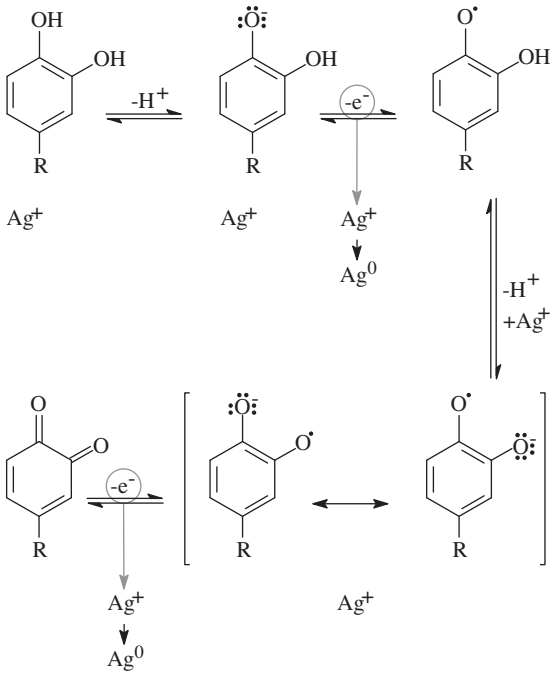

Fig. 1. Tentative mechanism for reduction of Ag^+ by polyphenols having two hydroxy groups in *ortho*-position.

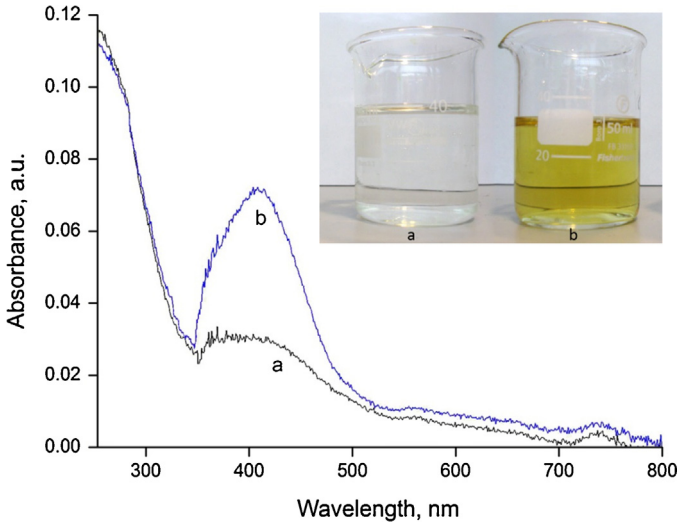

Fig. 2. UV–vis spectra of (a) starting solution and (b) solution of Ag NPs after 3 h of reaction. Inset: photograph of corresponding solutions.

to related quinone functionalities [37]. The tentative reduction mechanism of silver ions (Ag^+) to metallic silver (Ag^0) is illustrated in Fig. 1. The growth of silver metal to Ag NPs is also controlled by the interaction of the silver clusters with the surrounding hydroxy and quinone groups.

Reduction of aqueous Ag^+ ions during exposure to the extracted dye was followed by UV/vis spectroscopy. In Fig. 2, UV/vis spectra of solution containing 50 ppm of silver ions and extract of dye (dye-to-silver ratio $R_{dye/Ag} = 0.1$) at the beginning of reaction ($t = 0$) and after 3 h of stirring at room temperature is shown. After 3 h, a prominent peak appeared at 403 nm (Fig. 2b). The appearance of such a band in UV/vis spectrum is a consequence of the excitation of surface plasmon resonance band (SPR) of AgNPs [38]. The photograph of solutions on the beginning of reaction ($t = 0$) and after 3 h is shown as inset in Fig. 2. Transformation from completely transparent

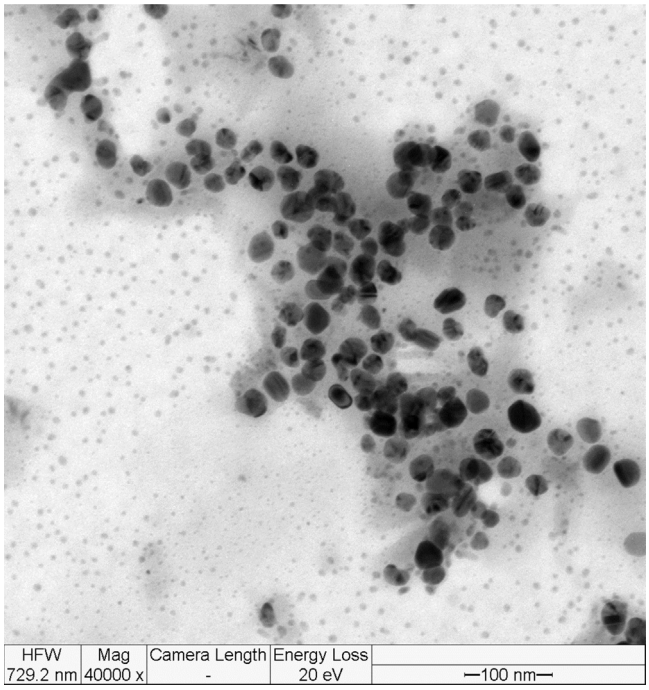

Fig. 3. TEM image of synthesized Ag NPS (50 ppm Ag solution, $R_{dye/Ag}$ = 0.1, reaction time 1 h).

colorless solution in t = 0 to transparent yellow colored solution after 3 h of reaction is clearly seen. It is well-known that colloidal silver nanoparticles exhibit yellowish-brown color in water [35,36].

The TEM image of AgNPs is shown in Fig. 3. A large number of particles with almost bimodal size distribution (bunch of bigger particles on the top of small particles) were observed. The shape of the particles is nearly spherical. The bimodal size distribution is characterized by a particle fraction having diameters of 17–30 nm and a fraction of smaller particles having sizes of 3–7 nm.

Dynamic light scattering measurement showed that the mean hydrodynamic diameter (z average) of nanoparticles was found to be 98, 92 and 23 nm for $R_{Dye/Ag}$ of 0.1, 1 and 10, respectively. Further increase of dye to Ag ratio did not resulted in a decrease in size of AgNPs. A decrease in hydrodynamic diameter of synthesized AgNPs indicates that extracted dye is able to act as a stabilizer and control size of particles. Other reason for the decrease in hydrodynamic diameter of synthesized AgNPs could be related to the higher reduction ability of dye in presented higher content. On the other hand, increasing in dye concentration has resulted into an increase in polydispersity index of 0.154, 0.262 and 0.545 for $R_{Dye/Ag}$ of 0.1, 1 and 10, respectively. The size analyzer is able to recognize dye molecules as a particle in the condition of the higher dye to silver nitrate concentration ratio. For higher $R_{Dye/Ag}$ ratios, there are more dye molecules with different sizes from AgNPs and therefore polydispersity index is increased.

The effect of $R_{Dye/Ag}$ on the Zeta potential of AgNPs was also investigated. Zeta potential was measured to around −21, −46 and −49 for $R_{Dye/Ag}$ of 0.1, 1 and 10, respectively. Increasing $R_{Dye/Ag}$ up to 10 resulted in a higher negative potential on the surfaces of the particles. Under these conditions, particles seemed to be fairly stable due to their electrostatic repulsion. This fact indicates that dye molecule act as a stabilizer.

3.2. Antibacterial activity in solution

The results of qualitative antibacterial assay revealed that the diameter of inhibition zone of 18.2, 17.5 and 0 nm for $R_{Dye/Ag}$ of 0.1, 1 and 10, respectively. The best antibacterial properties, confirmed by the larger inhibition zone of bacterial growth, were achieved with ratio $R_{Dye/Ag}$ = 0.1. Increasing dye concentration to $R_{Dye/Ag}$ = 1, a decrease in the inhibition zone diameter was observed. However, no inhibition zones was seen for the AgNPs prepared using $R_{Dye/Ag}$ = 10 that could be the consequence of encapsulation of AgNPs which finally led to lower diffusion of AgNPs on the agar plate.

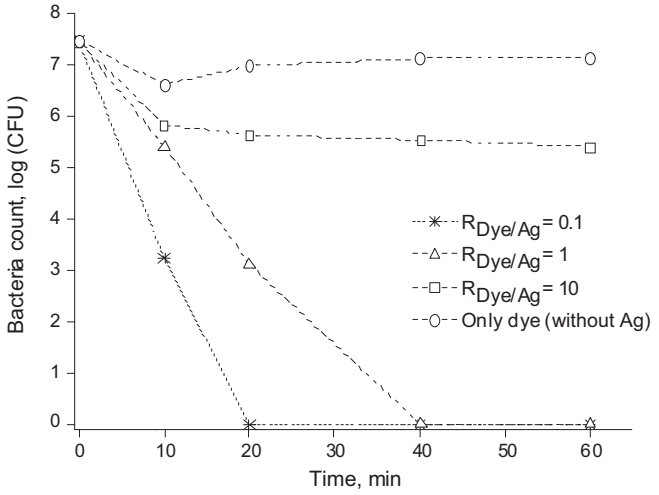

Fig. 4. Changes in number of bacteria in solution with various $R_{Dye/Ag}$.

The minimum bactericidal concentration (MBC) of synthesized AgNPs was measured to 20, 30 and higher than 40 ppm for $R_{Dye/Ag}$ of 0.1, 1 and 10, respectively. It was observed that at higher $R_{Dye/Ag}$ values, higher concentrations of AgNPs are needed for efficient antibacterial effect.

Fig. 4 shows bacteria count reduction in solution with various $R_{Dye/Ag}$ values during 60 min. As can be seen, increasing of the $R_{Dye/Ag}$ value led to a lower bactericidal rate, i.e. longer bacterial inactivation time indicating that higher concentration of dye causes slower release of silver nanoparticles to the medium. The bacteria reduction in solution without silver was not sensible after 1 h.

3.3. Application of AgNPs to wool fabrics

In order to provide wool fabrics with antibacterial properties, AgNPs were synthesized in solution with ratios $R_{Dye/Ag}$ = 0.1 and 1 loaded on wool fabrics. The silver contents of loaded samples obtained from EDX measurements is 1.256% and 0.767% for $R_{Dye/Ag}$ = 0.1 and 1, respectively. An increase in dye to silver ratio concentration resulted in lower deposition of AgNPs on wool fabric.

Fig. 5 shows the Zeta potential values of untreated wool fabrics determined in dependence of pH values of an aqueous KCl solution. The shape of the function is typical for a surface, where the charge-determining ions H^+ and OH^- were preferably adsorbed. That means the surface has no or only a few functional groups, which can undergo dissociation reactions in the presence of OH^- ions. At low pH values (pH < 4.4) adsorbed H^+ ions cause to a positive net surface charge and corresponding positive Zeta-potential values were determined. With increasing the pH value of the KCl solution the adsorption of OH^- ions is driven. Adsorbed OH^- ions compensated the positive surface charges and turned the sign of the net surface charge to negative. The pH value where the Zeta-potential is zero is called isoelectric point (IEP = $pH|_{\zeta=0}$). According to the Stern theory the IEP corresponds with the pH value of the fabric surface [39]. The isoelectric point of untreated wool fabric was observed at $pH|_{\zeta=0}$ 4.44 (Fig. 5). The absolute value of Zeta potential for AgNPs synthesized at $R_{Dye/Ag}$ = 1 is two-fold higher than that

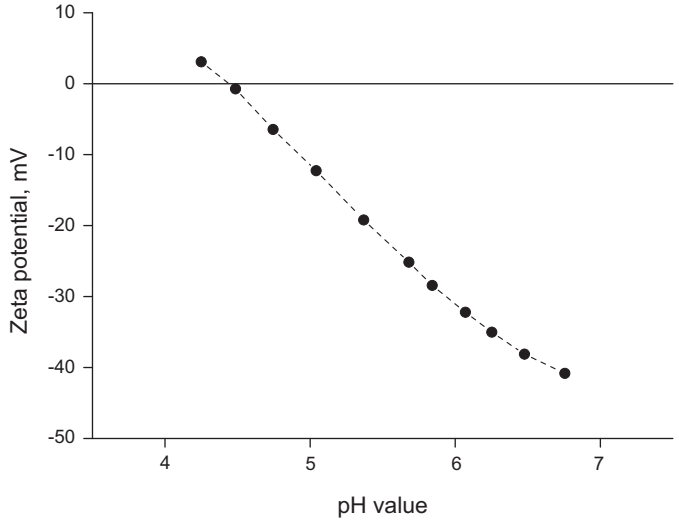

Fig. 5. Zeta potential values of untreated wool fabric in dependence of pH values of an aqueous 1 mmol/L KCl solution.

for samples synthesized at $R_{Dye/Ag} = 0.1$. Taking into account that the pH value that was used for exhaustion of AgNPs onto wool fabric was higher than isoelectric point of wool fabric, the negatively charged AgNPs with the ratio $R_{Dye/Ag} = 1$ repelled stronger and were adsorbed less onto wool. If it is assumed that the adsorption of AgNPs is driven by the formation of coordinative bonds to sulfur-containing groups on the wool surface the possible encapsulation of AgNPs with dye molecules in the presence of higher dye concentration would also reduce the degree of adsorption.

The surface morphology of the wool fabrics has been examined by SEM. Silver nanoparticles ($d \sim 90$ nm), adsorbed on the surface of wool fibers were observed independently of starting ratio $R_{Dye/Ag}$.

3.4. XPS results

The application of AgNPs having antibacterial activity does not only require the complete conversion of the ionic silver species into metallic silver, AgNPs must also be irreversibly fixed on the wool fiber surface. In order to analyze the oxidation state of AgNPs and studying their binding mechanisms to the wool fiber, surface high-resolution XPS element spectra were recorded. Wide-scan XPS spectra (not shown) taken from bare wool samples showed that the fiber surface is mainly composed from carbon, nitrogen, oxygen, and sulfur. The amount of sodium and calcium was too small to be determined accurately.

Fig. 6 compares characteristic high-resolution element XPS spectra of bare wool (Fig. 6a) and wool loaded with AgNPs (Fig. 6b). According to their shapes, the C 1s spectra of the two samples seemed to be not very different. They were deconvoluted into five component peaks showing the different binding states of the carbon atoms. The intensive component peaks *A* resulted from hydrocarbons (C_xH_y). Component peaks *E* (BE ≈ 289 eV) indicated the presence of carbonyl carbon atoms bonded as carboxylic acids (O═C—OH) and/or carboxylic esters (O═C—O—C). In the case of ester groups, the alcohol-sided carbon atoms (O═C—O—C) were observed as component peak *C* (BE ≈ 286.6 eV). Additionally, component peaks *C* show other C–O bonds, which are constituents of alcohol (C–OH) and ether groups (C–O–C). Carbonyl carbon atoms of amide groups (peptide bonds O═C—NH—C) were analyzed as component peak *D* (BE ≈ 288.2 eV). Photoelectrons from the corresponding amine-sided carbon atoms (O═C—NH—C), C–N bonds of amino groups, C–S bonds and carbon atoms, which are in α-position to the carbonyl carbons of carboxylic acid or ester groups (C–COO) contributed to component peak *B* (BE ≈ 285.9 eV).

In the case of a considerable amount of amino groups on the sample surface, the N 1s spectrum should show two component peaks because the binding energy values of protonated (C–N^+H) and non-protonated amino groups (C–N) is significantly different. Surprisingly, the N 1s spectrum of the bare wool fabric showed only one component peak *K* at BE = 400.2 eV (Fig. 6a). The small

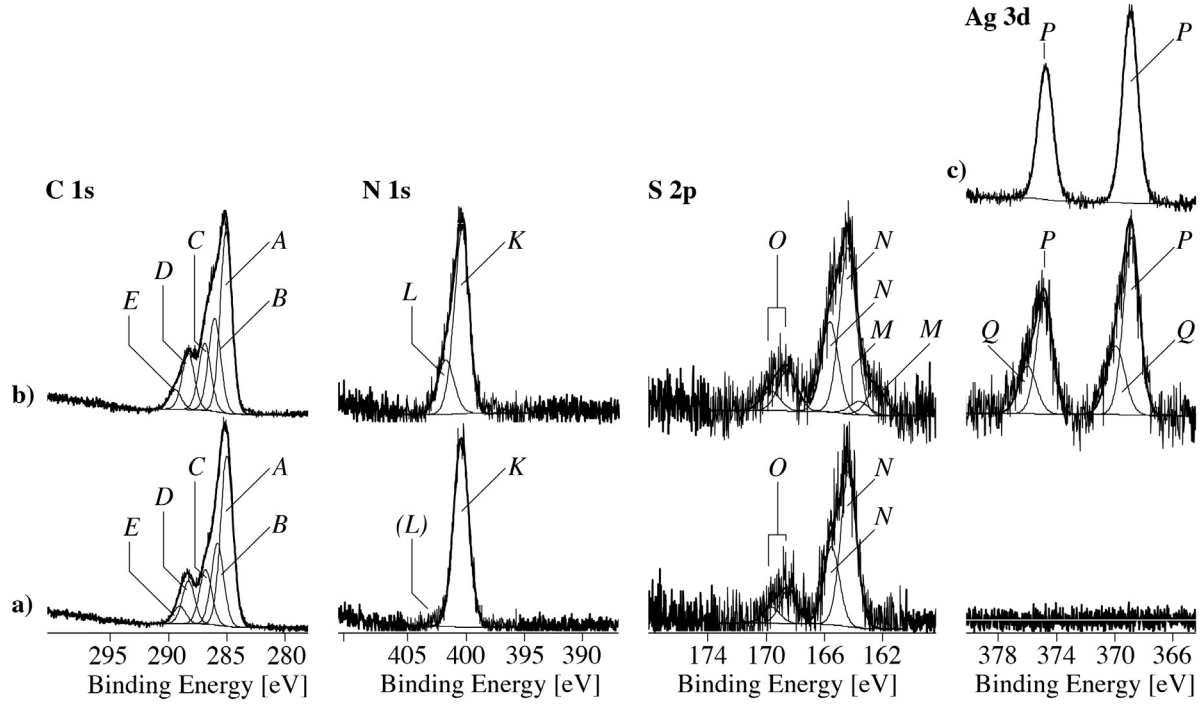

Fig. 6. High-resolution XPS element spectra (C 1s, N 1s, S 2p, and Ag 3d spectra) recorded from (a) a bare wool fabric sample and (b) a fabric sample loaded with AgNPs ($R_{Dye/Ag} = 0.1$). The Ag 3d spectrum (c) was recorded as reference spectrum from a silver foil.

shoulder assigned with *L* in brackets is not significant, but it could indicate the presence of a small amount of nitrogen atoms, which are bonded as amines. Obviously, the majority of all nitrogen atoms are involved in peptide bonds (amide groups), which are not subjected by a protonation equilibrium. After loading the wool fabric with AgNPs, the N 1s spectrum clearly showed a second component peak *L*, which is shifted to a higher binding energy value of about 1.3 eV. It is assumed that the additional component peak *L* resulted from strong chemical interactions between nitrogen-containing functional groups and the metallic AgNPs attached. The amide group is able to act as electron pair donator because it is characterized by a high electron density and the ability to transfer the electron density by its free electron pair to a silver atom acting as electron pair acceptor. The coordinative bonds formed in this way positivize the nitrogen atoms of the amide groups and shift their binding energy value to the binding energy value, which was observed as component peak *L*.

Beside the coordinative interactions between the amide groups and AgNPs is also able to form stable bonds to sulfur-containing functional groups. Due to the spin-orbit effect all S 2p spectra are split into the S $2p_{3/2}$ and S $2p_{1/2}$ spectra. The difference of the binding energy values $\Delta BE = BE[S\ 2p_{3/2}] - BE[S\ 2p_{1/2}] = 1.18$ eV and their intensity ratio of $[S\ 2p_{3/2}]:[S\ 2p_{1/2}] = 2:1$ were found as expected. As can be seen in Fig. 6a, the bare wool surface contains sulfur, which is bonded in two different states. Component peak *N* ($BE[S\ 2p_{3/2}] = 163.96$ eV) arose from organically bonded sulfur, here preferably as the constituent of dithiol groups (C–S–S–C) of cysteine. The second component peak *O* ($BE[S\ 2p_{3/2}] = 168.14$ eV) resulted from sulfate groups (SO_4^{2-}). After loading the wool with Ag NPs a third component peak *M* was observed at $BE[S\ 2p_{3/2}] = 162.01$ eV (Fig. 6b). The binding energy for this component peak is very typical for Ag_2S [40]. These findings are supported by the well-known high driving force of silver to form insoluble salts. Compared to the Ag 3d reference spectrum recorded from a silver foil (Fig. 6c), which is characterized by only one component peak *P* ($BE[Ag\ 3d_{5/2}] = 368.5$ eV), the Ag 3d spectrum of the wool fabric loaded with AgNPs clearly shows two component peaks (Fig. 6b). Although the binding energy value found for component peak *P* was slightly higher than the reference value, which is given for freshly sputtered silver samples to calibrate XPS spectrometers, it is clear that component peak *P* appeared from metallic silver (Ag^0). The second component peak *Q* ($BE[Ag\ 3d_{5/2}] = 369.5$ eV) obviously resulted from silver atoms, which are involved in strong interactions to the functional groups of the wool fiber surface. The binding energy value of the component peak Ag $3d_{5/2}$ *Q* was also slightly higher as the value expected for Ag_2S [33] or silver atoms bonded to organic sulfides (the binding energy values referred in [33] were determined from silver attached to poly(*p*-phenylene sulfide), which is characterized by a high π-electron density along the polymer backbone).

The XPS findings showed that AgNPs are fixed on the wool surface by strong chemical interactions. While the reaction of silver atoms and organic sulfides is necessarily accompanied by a partial oxidation of the AgNPs, the metallic state of the silver atoms was kept by the formation of coordinative bonds between nitrogen-containing surface groups and AgNPs.

3.5. Effect of pH and temperature on loading of AgNPs on wool

The results show that amount of silver at lower pH are higher. The pH effect can be understood by considering that at pH higher than isoelectric point wool fibre has a negative surface charge, which would act as an initial deterrent to sorption of anionic species, such as AgNPs used in this study. At pH 3, a considerable proportion of internal amino groups are protonated, leading to a neutralization of this surface charge and absorption of higher amount AgNPs. There is also a dependency of silver loaded on the wool surface on temperature. The silver contents on the wool fibres treated by AgNPs from the sample with $R_{Dye/Ag} = 1$ at pH 3 and at temperature of 25, 45 and 65 °C is 0.781, 0.808, respectively. For the same dye to silver ratio, but at pH 5, the silver content is 0.768, 0.78 and 0.847% for wool samples treated at 25, 45 and 65 °C, respectively. It is apparent, that an increase in temperature resulted in higher load of silver on the fabrics. This can be expected due to the higher kinetic energy of the system at higher temperature. In Fig. 7, SEM images of loaded samples at 25 and 65 °C are shown. In these micrographs, higher loading of particles on the surface of wool fibers at higher temperature was observed.

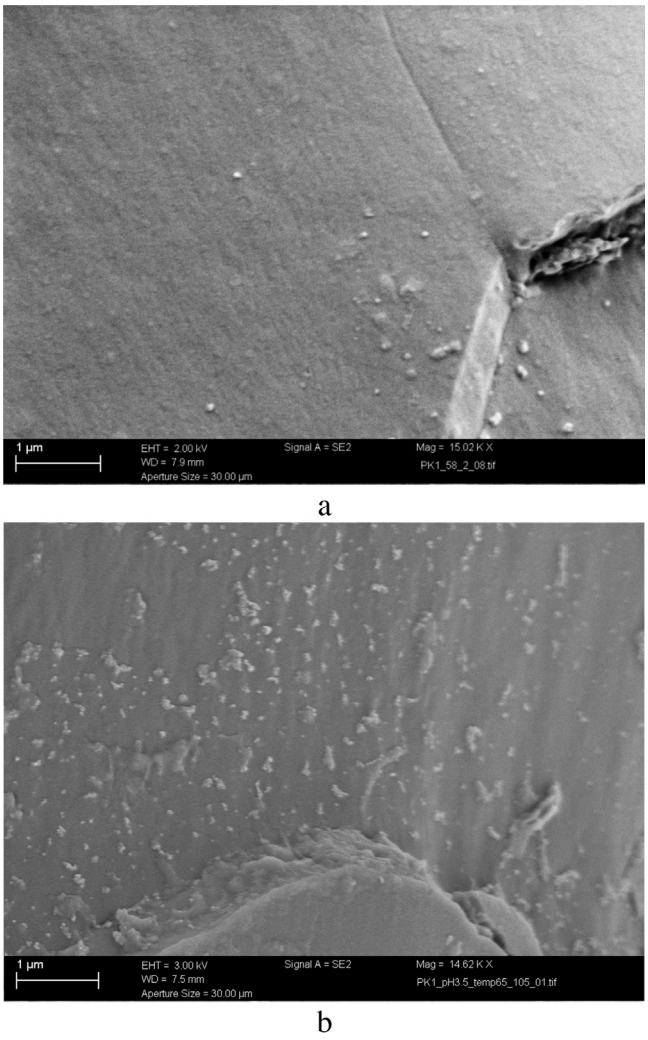

Fig. 7. SEM micrographs of loaded wool fabric with AgNPs at (a) 25 °C and (b) 65 °C.

3.6. Antibacterial activity of wool fabric loaded with AgNPs

Antibacterial efficiency of wool fabrics loaded with Ag NPs before and after five washing cycles is presented in Table 1. The antibacterial efficiency of the loaded sample in all cases was excellent, independently of the dye to silver ratio applied. The untreated wool sample ($R_{Dye/Ag} = 0$), as expected, does not show any antibacterial capability and the number of bacteria increased after 24 h. After repeated washing cycles the antibacterial efficiency of loaded wool samples didn't changed.

Table 1
Antibacterial test results of the loaded wool with AgNps.

Wool fabric's surface state	$R_{Dye/Ag}$	Initial number of bacterial colonies (CFU)	Final number of bacterial colonies (CFU)
Before washing	0	1.83×10^5	3.81×10^7
	0.1	1.93×10^5	<10
	1	1.90×10^5	<10
After five washing cycles	0	1.89×10^5	2.13×10^7
	0.1	2.10×10^5	<10
	1	1.93×10^5	<10

4. Conclusions

The biosynthesis of silver nanoparticles using Pomegranate peel extract as a reducing agent was presented. The dye to silver ratio was the influencing factor for size, polydispersity and antibacterial properties of synthesized nanoparticles. Increasing dye concentration led to decrease in the direct contact of AgNPs, i.e. antibacterial agent with the bacterial cell membrane which lowered the killing rate of bacteria. To obtain antimicrobial properties the dye to silver ratio was optimized. Synthesized AgNPs were applied on wool by exhaustion method. The adsorption of nanoparticles on wool was dependent on electrostatic interactions and it was increased at lower pH conditions in which there are fewer anionic groups on the wool fibre. Increasing temperature during treatment resulted in higher adsorption of nanoparticles on wool. Antibacterial activity of samples was checked against *E. coli* bacteria and the AgNPs treated fabrics demonstrated good antibacterial capability even after several washing cycles. XPS studies have demonstrated that silver nanoparticles are attached to the keratin fibers as a result of the interaction between silver and sulfur.

Acknowledgments

The studies are related to the activity of the European network action COST Action MP1106 "Smart and Green Interfaces – from Single Bubbles and Drops to Industrial, Environmental and Biomedical Applications" and COST Action CM1101 "Colloidal Aspects of Nanoscience for Innovative Processes and Materials".

References

[1] R. Dastjerdi, M. Montazer, A review on the application of inorganic nano-structured materials in the modification of textiles: focus on anti-microbial properties, Colloids Surf. B: Biointerfaces 79 (2010) 5.
[2] V. Ilic, Z. Šaponjic, V. Vodnik, D. Mihailovic, P. Jovancic, J. Nedeljkovic, M. Radetic, The study of coloration and antibacterial efficiency of corona activated dyed polyamide and polyester fabrics loaded with Ag nanoparticles, Fibers Polym. 10 (2009) 650.
[3] T.M. Tolaymat, A.M. El Badawy, A. Genaidy, K.G. Scheckel, T.P. Luxton, M. Suidan, An evidence-based environmental perspective of manufactured silver nanoparticle in syntheses and applications: A systematic review and critical appraisal of peer-reviewed scientific papers, Sci. Total Environ. 408 (2010) 999.
[4] M. Nasiri Boroumand, M. Montazer, V. Dutschk, Biosynthesis of silver nanoparticles using *Reseda luteola* L. and their antimicrobial activity, Ind. Tex. 64 (2013) 123.
[5] H.R. Ghorbani, A.A. Safekordi, H. Attar, S.M. Sorkhabadi, Biological and non-biological methods for silver nanoparticles synthesis, Chem. Biochem. Eng. Quart. 25 (2011) 317.
[6] J.L. Gardea-Torresdey, E. Gomez, J.R. Peralta-Videa, J.G. Parsons, H. Troiani, M. Jose-Yacaman, Alfalfa sprouts: a natural source for the synthesis of silver nanoparticles, Langmuir 19 (2003) 1357.
[7] A. Saxena, R.M. Tripathi, R.P. Singh, Biological synthesis of silver nanoparticles by using onion (*Allium cepa*) extract and their antibacterial activity, Digest J. Nanomater. Biostruct. 5 (2010) 427.
[8] V. Kumar, S.K. Yadav, Plant-mediated synthesis of silver and gold nanoparticles and their applications, J. Chem. Technol. Biotechnol. 84 (2009) 151.
[9] W.K. Jung, H.C. Koo, K.W. Kim, S. Shin, S.H. Kim, Y.H. Park, Antibacterial activity and mechanism of action of the silver ion in *Staphylococcus aureus* and *Escherichia coli*, Appl. Environ. Microbiol. 74 (2008) 2171.
[10] S.H. Kim, H.S. Lee, D.S. Ryu, S.J. Choi, D.S. Lee, Antibacterial activity of silver-nanoparticles against *Staphylococcus aureus* and *Escherichia coli*, Korean J. Microbiol. Biotechnol. 39 (2011) 77.
[11] H.J. Lee, S.Y. Yeo, S.H. Jeong, Antibacterial effect of nanosized silver colloidal solution on textile fabrics, J. Mater. Sci. 38 (2003) 2199.
[12] H.J. Lee, S.H. Jeong, Bacteriostasis of nanosized colloidal silver on polyester nonwovens, Textile Res. J. 74 (2004) 442.
[13] N. Durán, P.D. Marcato, G.I.H. De Souza, O.L. Alves, E. Esposito, Antibacterial effect of silver nanoparticles produced by fungal process on textile fabrics and their effluent treatment, J. Biomed. Nanotechnol. 3 (2007) 203.
[14] S.K. Bajpai, M. Bajpai, L. Sharma, M.M. Yallapu, Silver nanoparticles loaded thermosensitive cotton fabric for antibacterial application, J. Ind. Textiles 0 (2013) 1.
[15] T. Yuranova, A.G. Rincon, A. Bozzi, S. Parra, C. Pulgarin, P. Albers, J. Kiwi, Antibacterial textiles prepared by RF-plasma and vacuum-UV mediated deposition of silver, J. Photochem. Photobiol. A: Chem. 161 (2003) 27.
[16] N. Yang, W.H. Li, Mango peel extract mediated novel route for synthesis of silver nanoparticles and antibacterial application of silver nanoparticles loaded onto non-woven fabrics, Ind. Crops Prod. 48 (2013) 81.
[17] S.Y. Yeo, S.H. Jeong, Preparation and characterization of polypropylene/silver nanocomposite fibers, Polym. Int. 52 (2003) 1053.
[18] V. Allahyarzadeh, M. Montazer, N. Hemmati Nejad, N. Samadi, In situ synthesis of nano silver on polyester using NaOH/Nano TiO2, J. Appl. Polym. Sci. 129 (2013) 892.
[19] M.D. Teli, J. Sheikh, Nanosilver containing grafted bamboo rayon as antibacterial material, Fibers Polym. 13 (2012) 1280.
[20] M. Pollini, F. Paladini, A. Licciulli, A. Maffezzoli, L. Nicolais, A. Sannino, Silver-coated wool yarns with durable antibacterial properties, J. Appl. Polym. Sci. 125 (2012) 2239.
[21] L. Hadad, N. Perkas, Y. Gofer, J.C. Moreno, A. Ghule, A. Gedanken, Sonochemical deposition of silver nanoparticles on wool fibers, J. Appl. Polym. Sci. 104 (2007) 1732.
[22] H. Barani, M. Montazer, N. Samadi, T. Toliyat, In situ synthesis of nano silver/lecithin on wool: enhancing nanoparticles diffusion, Colloids Surf. B: Biointerfaces 92 (2012) 9.
[23] B. Tang, J. Wang, S. Xu, T. Afrin, W. Xu, L. Sun, X. Wang, Application of anisotropic silver nanoparticles: multifunctionalization of wool fabric, J. Colloid Interface Sci. 356 (2011) 513.
[24] H.Y. Ki, J.H. Kim, S.C. Kwon, S.H. Jeong, A study on multifunctional wool textiles treated with nano-sized silver, J. Mater. Sci. 42 (2007) 8020.
[25] P.S. Rad, M. Montazer, M.K. Rahimi, Simultaneous antimicrobial and dyeing of Wool: a facial method, J. Appl. Polym. Sci. 122 (2011) 1405.
[26] D.G. King, A.P. Pierlot, Absorption of nanoparticles by wool, Color. Technol. 125 (2009) 111.
[27] M. Montazer, A. Behzadnia, E. Pakdel, M.K. Rahimi, M.B. Moghadam, Photo induced silver on nano titanium dioxide as an enhanced antimicrobial agent for wool, J. Photochem. Photobiol. B: Biol. 103 (2011) 207.
[28] H.J. Lee, S.Y. Yeo, S.H. Jeong, Antibacterial effect of nanosized silver colloidal solution on textile fabrics, J. Matera. Sci. 38 (2003) 2199.
[29] S.S. Kulkarni, A.V. Gokhale, U.M. Bodake, G.R. Pathade, Cotton dyeing with natural dye extracted from Pomegranate (*Punica granatum*) peel, Univ. J. Environ. Res. Technol. 1 (2011) 135.
[30] H.M. Yehia, M.F. Elkhadragy, A.E. Abdel Moneim, Antimicrobial activity of pomegranate rind peel extracts, Afr. J. Microbiol. Res. 4 (2011) 3664.
[31] T. Thirumurugan, K. Kuldeep, Biological synthesis and characterization of gold nanoparticles from pomegranate, Int. J. Future Biotechnol. 2 (2013) 1.
[32] A.V. Delgado, F. González-Caballero, R.J. Hunter, L.K. Koopal, J. Lyklema, Measurement and interpretation of electrokinetic phenomena (IUPAC Technical Report), Pure Appl. Chem. 77 (2005) 1753.
[33] H.J. Jacobasch, Characterization of solid surfaces by electrokinetic measurements, Prog. Org. Coat. 17 (1989) 115.
[34] D.A. Shirley, High-resolution X-ray photoemission spectrum of the valence bands of gold, Phys. Rev. B 5 (1972) 4709.
[35] H. Barani, M. Montazer, N. Samadi, T. Tolyat, Synthesis of Ag-liposome nano composites, J. Liposome Res. 20 (2010) 323.
[36] H. Barani, M. Montazer, N. Samadi, T. Tolyat, Nano silver entrapped in phospholipids membrane: synthesis characteristics and antibacterial kinetics, Mol. Membr. Biol. 28 (2011) 206.
[37] N. Roy, S. Mondal, R.A. Laskar, S. Basu, D. Mandal, N.A. Begum, Biogenic synthesis of Au and Ag nanoparticles by Indian propolis and its constituents, Colloids Surf. B: Biointerfaces 76 (2010) 317.
[38] P. Mulvaney, Surface plasmon spectroscopy of nanosized metal particles, Langmuir 12 (1996) 788.
[39] O. Stern, Zur theorie der elektrolytischen Doppelschicht, Z. Elektrochemie 30 (1924) 508.
[40] L.J. Gerenser, K. Goppert-Berarducci, R.C. Baetzold, J.M. Pochan, The application of photoemission, molecular orbital calculations, and molecular mechanics to the silver-poly(p-phenylene sulfide) interface, J. Chem. Phys. 95 (1991) 4641.